



BRNO UNIVERSITY OF TECHNOLOGY

VYSOKÉ UČENÍ TECHNICKÉ V BRNĚ

FACULTY OF MECHANICAL ENGINEERING

FAKULTA STROJNÍHO INŽENÝRSTVÍ

INSTITUTE OF AEROSPACE ENGINEERING

LETECKÝ ÚSTAV

FATIGUE CRACK GROWTH RETARDATION TECHNIQUES FOR THE INTEGRAL AIRFRAME STRUCTURE

FATIGUE CRACK GROWTH RETARDATION TECHNIQUES FOR THE INTEGRAL AIRFRAME STRUCTURE

DOCTORAL THESIS

DIZERTAČNÍ PRÁCE

AUTHOR

AUTOR PRÁCE

Ing. Václav Jetela

SUPERVISOR

ŠKOLITEL

doc. Ing. Josef Klement, CSc.

BRNO 2022

Abstract

A problem with fast crack propagation arose from utilizing integral airframe structure. One of the techniques to slow down crack propagation and prolong the fatigue life is the application of crack retarder. The aim of this thesis is to compare the performance of additively manufactured crack retarders with bonded ones in terms of the fatigue life, crack growth rate and delamination. In case of the bonded crack retarders; no attention has been paid to the crack retarders made of stainless steel. The stainless steel appears to be a suitable candidate for its coefficient of thermal expansion close to the aluminum, high strength and elastic modulus. Regarding the additively manufactured crack retarders, little or no attention has been paid to the crack retarders made of metals different than the base structure.

To address this research gap, two distinctive technologies were selected: cold spray and ultrasonic consolidation. Using the cold spray, the titanium and stainless steel crack retarders were deposited. Using the ultrasonic consolidation, the stainless steel crack retarders were welded. In the experimental work, the crack advance was visually observed. The crack retarder delamination was monitored using the pulsed thermography with subsequent Thermographic Signal Reconstruction. Bonded stainless steel crack retarders proved to be a suitable alternative to the already proven carbon fibre crack retarders. Stainless steel retarders significantly lowered the fatigue crack growth rate which resulted in longer fatigue life. However, all cold sprayed crack retarders accelerated crack growth rate and led to the specimen's premature failure. Ultrasonically consolidated crack retarder with two steel layers was the most effective in the life prolongation. The study also proved, that the delamination in the ultrasonically consolidated metal laminates can be detected using pulsed thermography.

Keywords: Selective reinforcement, Bonded Crack Retarder, Cold Spray, Ultrasonic Consolidation, Crack growth, Damage Tolerance, Thermography, Delamination.

Abstrakt

Únavová trhлина roste v integrální konstrukci rychleji než v konstrukci nýtované. Tento problém se projevuje výrazně nižší životností integrální konstrukce. Jednou z metod jak omezit růst dlouhých únavových trhlin je aplikace lokálního vyztužení, tzv. zastavovače trhliny. Zastavovač omezuje rozevření čela trhliny, čímž výrazně zpomaluje její růst.

V první části práce jsou kriticky hodnoceny dosavadní studie zabývající se metodami zpomalování růstu dlouhých únavových trhlin. Rešerše je rozšířena i na technologie, které materiál nepřidávají, ale například pouze mění stav materiálu podkladové konstrukce. Studie jsou hodnoceny s ohledem na použité technologie, materiály a zvýšení únavové životnosti. Rovněž jsou zmíněny obecné závěry týkající se požadavků na vlastnosti optimálního zastavovače trhlin. Na konci rešerše jsou diskutovány směry, kterými by se mohl ubírat výzkum v oblasti zpomalování růstu dlouhých únavových trhlin.

Na základě zjištěných mezer v současném stavu poznání byl stanoven cíl práce; porovnat dopad lepených a aditivně vyrobených zastavovačů na růst trhliny v konstrukci z hliníkové slitiny. Přičemž byly vybrány tyto aditivní technologie: cold spray a ultrazvuková konsolidace. Obě tyto technologie umožňují vytvořit vysokopevnostní spoj mezi nestejnými kovovými materiály, čímž by bylo možné minimalizovat rozvoj delaminace mezi zastavovačem a podkladovou konstrukcí. Z hlediska materiálů se práce zaměřuje zejména na vysokopevnostní nerezovou ocel z těchto důvodů: vysoká pevnost, vysoký modul pružnosti v tahu a koeficient tepelné roztažnosti blízký hliníkové slitině. Pro potřeby porovnání byly do studie zahrnuty i lepené zastavovače z uhlíkového kompozitu a stříkané zastavovače z titanové slitiny.

Teoretická část práce poskytuje vhled do lineární lomové mechaniky a šíření dlouhých únavových trhlin. Rovněž jsou diskutovány efekty mající dopad na růst únavových trhlin v kovových konstrukcích. V kapitole jsou také představeny jednotlivé technologie použité pro výrobu zastavovačů trhlin v této práci. V závěru kapitoly jsou podrobně rozebrány mechanismy a vlastnosti zastavovačů trhliny, které mají pozitivní i negativní dopad na rychlost šíření trhliny v podkladové konstrukci.

V experimentální části práce je nejprve popsána výroba vzorků se zastavovači trhlin. V případě lepených zastavovačů byly použité v minulosti osvědčené postupy úpravy adherendů. V případě zastavovačů stříkaných metodou cold spray byly použity v minulosti optimalizované procesní parametry nástřiku. Pro výrobu ultrazvukově konsolidovaných zastavovačů bylo nezbytné provést optimalizaci procesních parametrů, protože jejich hodnoty nebyly pro danou aplikaci ověřené. Připravené vzorky byly podrobeny cyklickému zatížení při němž se opticky pozoroval vznik a následný růst únavové trhliny. Za účelem zachycení delaminace byla vyztužená strana vzorku snímána termokamerou. Termokamera snímala teplotní odezvu vzorku po optické excitaci. Termogramy byly dále zpracovávány metodou rekonstrukce termografického signálu za účelem zvýšení kontrastu delaminace.

Měřeními bylo prokázáno, že zastavovače z nerezové oceli významně prodloužují životnost hliníkové konstrukce a snižují rychlost šíření trhliny. To platí pro zastavovače lepené a ultrazvukově konsolidované. Zastavovače z titanové slitiny a nerezové oceli vyráběné metodou cold spray nebyly efektivní. Jejich aplikace na podkladovou konstrukci vedla ke snížení únavové životnosti a zvýšení rychlosti šíření únavové trhliny v podkladové konstrukci. Stříkané zastavovače nedelaminovaly; únavová trhlina prorostla přímo do zastavovačů trhlin. K přímému růstu trhliny do zastavovače došlo i v případě vzorku s ultrazvukově konsolidovanými zastavovači. Zastavovače ze dvou vrstev oceli umožnily zpomalit růst únavové trhliny nejvíce. Zastavovač v tomto případě delaminoval. Přičemž závislost velikosti delaminace na počtu cyklů má stejný trend jako v případě zastavovačů lepených.

Tato disertační práce porovnává dopad doposud nevyzkoušených materiálů zastavovače a výrobních technologií na rychlost šíření trhliny v hliníkové konstrukci, delaminaci zastavovače a životnost vzorku. Výsledky studie je možné využít k tvorbě modelů predikujících růst trhliny v ultrazvukově konsolidovaných a lepených konstrukcích. Výsledky experimentálních měření navíc prokazují, že je možné detekovat delaminaci v ultrazvukově konsolidovaném laminátu metodou pulzní termografie.

Klíčová slova: Lokální vyztužení, Lepený zastavovač trhliny, Cold spray, Ultrazvuková konsolidace, Růst trhliny, Přípustné poškození, Termografie, Delaminace.

Contents

1	Introduction	7
1.1	Problem formulation	7
1.2	Justification of the problem	8
2	Aim and Objectives	9
3	Experimental Work	10
3.1	Substrate	10
3.2	Bonded crack retarders	13
3.3	Cold sprayed crack retarders	14
3.4	Consolidated crack retarders	15
3.5	Fatigue crack growth test	18
3.6	Delamination monitoring	19
3.7	Digital image processing	20
3.8	Results and discussion	20
4	Conclusion	30
4.1	Research implication and contribution	31
	References	33
	Curriculum Vitae	36

Chapter 1

Introduction

1.1 Problem formulation

The primary airframe structure may consists of stringers, skin and trusses. Riveting, a traditional technique to join these structural elements together, is being replaced by the integral airframe structures manufacturing. Besides the welded integral structures, where stringers are made separately and then welded to the separately manufactured skin, the integral panels can be extruded or high-speed machined. There, stringers and skin are made from one piece.

In comparison with the riveted structures, the integral airframe structures saves weight and contain less stress concentrators but do not contain the physical barriers against fatigue crack growth. The physical barrier is classified as a place in a structure where one part of a structure is covered by another part (Fig. 1.1). If the physical barriers are non-existent, the fatigue crack can grow from one part to another without a delay [1]. This results in the earlier fatigue failure of integral structure. Such problem can be expressed by the fatigue crack growth curve of both structures (Fig. 1.2).



Figure 1.1: A comparison of integral and riveted structures: Physical barrier marked with blue colour [1].

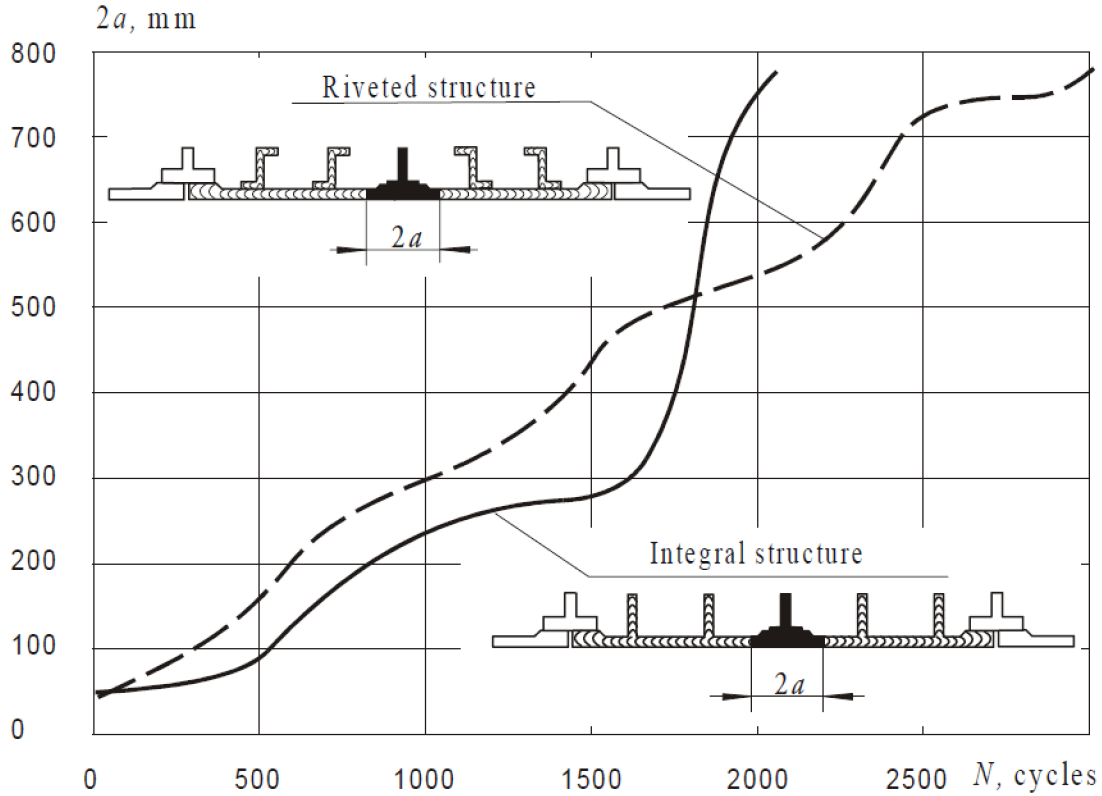


Figure 1.2: Duration of crack growth in riveted and integral panel skin from initial skin crack beneath broken central stringer [1].

1.2 Justification of the problem

According to the previous section, the integral airframe structure can be seen as a fatigue critical component. With respect to the study from 2002 [2], fatigue had contributed 55% towards aircraft service failures. Regulators are aware of it and thus penalize unitized structures by imposing an additional design safety factor [3]. By increasing the number of design safety factors, the aircraft structure becomes heavier. Considering these facts, it is even more important to cope with fatigue life extension of such structures to create greener aircraft.

Moreover, as the fatigue life extends, a decrease in the number of airframe inspections can be attained. It is desirable to reduce the number of inspections because: (1) the airframe maintenance occupies 30% of total aircraft maintenance cost and (2) the airframe maintenance cost per flight hour steadily increases as the aircraft ages [4].

Chapter 2

Aim and Objectives

The main aim of this thesis is to compare the impacts of bonded and additively manufactured crack retarders on the fatigue crack growth in the metallic structure. To address this aim, individual objectives are enumerated in subsequent points:

1. To measure the performance of steel bonded crack retarders. The 2024-T351 M(T) specimens with the AISI 301 bonded crack retarders will be prepared to perform the fatigue crack growth test incorporating delamination monitoring.
2. To measure the performance of additively manufactured crack retarders. The 2024-T351 M(T) specimens with the AISI 316L, Ti-6Al-4V cold sprayed crack retarders will be prepared to perform the fatigue crack growth test incorporating delamination monitoring. The 2024-T351 M(T) specimens with the AISI 301/Al crack retarders will be prepared to perform the fatigue crack growth test incorporating delamination monitoring.
3. To compare the bonded crack retarders with additively manufactured ones and find the most effective crack retarder in terms of life extension, weight and delamination resistance.

Chapter 3

Experimental Work

This chapter describes the experimental studies (Tab. 3.1) that have been done to meet the thesis objectives¹. Each following section is named after the technology used in crack retarder fabrication. In the end, crack retarders are evaluated in terms of crack growth rate, fatigue life extension, weight and delamination resistance.

3.1 Substrate

The M(T) specimens were high-speed milled from the sheet made of 2024-T351 aluminium alloy, which is widely used in various aerospace applications. The fatigue crack growth tests were carried out on the M(T) specimen with several geometries (Fig. 3.1). The bare specimens were used as a substrate for bonded crack retarders made of AISI 301, CF UD and cold sprayed crack retarders made of AISI 316L and Ti-6Al-4V. The M(T) specimen width and length were chosen according to ASTM E647 [5] while the thickness of 2 mm represented common integral wing skin panel. The mechanical properties of substrate are shown in Tab. 3.2. In case of the specimens with ultrasonically consolidated crack retarders, the substrate was manufactured in the reverse order (as elaborated in Chapter 3.4).

¹Specimens with thinner crack retarder are marked with "1" (e.g. 1-AISI301), thicker crack retarder are marked with "2" (e.g. 2-AISI301)

Table 3.1: Test matrix.

	Specimen name	Crack retarder constituents					Crack retarder				Substrate	Loading parameters	
		No. of layers	Layer	Thickness (t_{lay}) [mm]	No. of interlayers	Interlayer	Length [mm]	Width [mm]	Thickness (t_r) [mm]	Manufacturing temperature [°C]	Material and geometry	Dimensions [mm]	Maximum stress (σ_{max}) [MPa]
II	Bare	0	-	0	0	-	0	0	0	RT		60	$R = 0.1$ $f = 15$ Hz RT
	1-AISI301-BCR	1	AISI 301	0.26	1	Araldite® 2011	200	10	0.44	80		60	
	2-AISI301A-BCR	2	AISI 301	0.26	2	Araldite® 2011	200	10	0.60	80		60	
	2-AISI301B-BCR	2	AISI 301	0.26	2	Araldite® 2011	200	10	0.55	80		60	
	1-CFUD-BCR	2	M10R/38%/UD150/CHS	0.16	1	Araldite® 2011	200	10.2	0.53	80	2024-T351 M(T)	60	
	2-CFUD-BCR	5	M10R/38%/UD150/CHS	0.16	1	Araldite® 2011	200	10.2	1.08	80		60	
	1-AISI316L-CSCR	3	AISI 316L	0.20	0	-	200	11.1	0.48	?	375 x 100 x 2	60	
	2-AISI316L-CSCR	6	AISI 316L	0.20	0	-	200	11.2	0.96	?		60	
	1-Ti64-CSCR	3	Ti-6Al-4V	0.20	0	-	200	11.2	0.51	?	2024-T351 M(T)	60	
	2-Ti64-CSCR	6	Ti-6Al-4V	0.20	0	-	200	11.3	1.02	?		60	
	Bare	0	-	0	0	-	0	0	0	RT		60	
	1-AISI301-UCCR	1	AISI 301	0.26	1	1100-O	200	10.2	0.29	52		60	
	Bare	0	-	0	0	-	0	0	0	RT		100	
	2-AISI301-UCCR	2	AISI 301	0.26	2	1100-O	200	10.2	0.71	52		100	

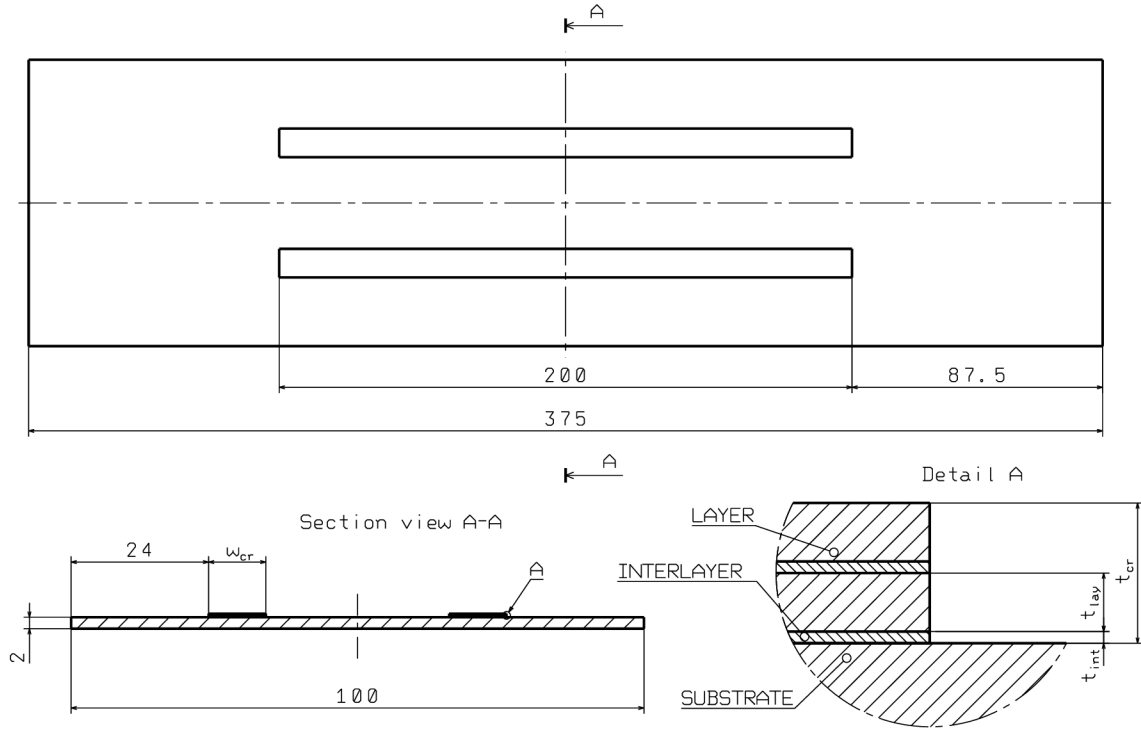


Figure 3.1: Specimen shape. Dimensions in mm, not in scale.

Table 3.2: Mechanical and thermal properties of substrate, bonded crack retarder and adhesive.

Material	2024-T351 ^a	AISI 301	M10R/38% /UD150/CHS	Araldite [®] 2011
E [GPa]	72.4	185 ^b	136 ^d /143 ^e	1.9 ^h
ρ [g/cm ³]	2.77	7.88 ^c	1.57 ^f	1.05 ^h
α [10^{-6} /K]	23	17 ^c	1 ^g	-
Rm [MPa]	470	1635 ^b	2168 ^d /2676 ^e	-
$Rp_{0.2}$ [MPa]	325	1508 ^b	-	-
A [%]	20	2.1 ^b	-	-

^a [6]

^b [7]

^c [8]

^d Two layers. Tested according to ASTM D3039.

^e Five layers. Tested according to ASTM D3039.

^f [9]

^g Typical generic values.

^h [10]

3.2 Bonded crack retarders

Substrate surface pretreatment: The FPL etching, commonly used surface preparation prior adhesive bonding in the aircraft industry, was performed on all M(T) specimens with bonded crack retarders. First, the surface was degreased with acetone and then FPL etched in the bath composed of $\text{Na}_2\text{Cr}_2\text{O}_7 \cdot 2\text{H}_2\text{O}$, H_2SO_4 and H_2O . The etching duration was four hours at the ambient temperature. Finally, the surface was rinsed with water and blow-dried with the 45 °C air.

3.2.1 Austenitic stainless steel

The capability of retarding the crack growth was examined for the specimen bonded with one steel layer and two steel layers². The AISI 301 austenitic stainless steel in the work-hardened state was chosen for its high strength, elastic modulus and CTE (see Tab. 3.2 for mechanical properties).

Crack retarder surface pretreatment: The straps used for adhesive bonding of crack retarders were cut out of the sheet made of 0.255 mm thick AISI 301 steel and degreased with acetone. After that, the straps were immersed in the solution containing 12.5% HF, 40.8% H_2O , and 46.7% HNO_3 for 20 minutes at the ambient temperature. In the end, rinsing with water and blow-drying with the 45 °C air took place.

Adhesive bonding: The crack retarders were bonded onto the specimen surface by the two-component Araldite[®] 2011 structural adhesive. The specimen with one steel layer (1-AISI301-BCR) was cured for 24 hours at the ambient temperature and for 30 minutes at the 80 °C. In case of the specimen with two steel layers (2-AISI301-BCR), first, two pretreated straps were bonded together and cured. An excessive adhesive layer on the outer surfaces was removed. Then, the resulting BCRs were degreased with acetone and immersed in the solution containing H_2O , HF and HNO_3 for 20 minutes at the ambient temperature. Finally, bonding onto the substrate and curing were done. The same curing process was used as in the case of the 1-AISI301-BCR.

²Two specimens with two steel layers were manufactured; specimen 2-AISI301A-BCR and 2-AISI301B-BCR (Tab. 3.1).

3.2.2 Unidirectional carbon fibre

To compare the performance of steel crack retarders with previously validated crack retarder material, the BCRs made of two and five layers of M10R/38%/UD150/CHS prepreg were prepared. The prepreg consists of the high-strength unidirectional 12K carbon fibre fabric and M10R epoxy resin matrix (see mechanical properties in Tab. 3.2).

Crack retarder manufacturing process: First, the prepreg roll was de-frozen at the ambient temperature to avoid the condensation of air humidity. Then, the individual prepreg plies were cut out of the prepreg roll. After removing the release film from the prepreg plies, the desired number of prepreg plies was positioned in a single direction. Then the entire assembly was covered with the peel ply, bleeder cloth and vacuum bagging film. Such assembly was autoclaved at 5 bar and 120 °C for 1 hour. Finally, the cured sheets were cut with a hand saw to obtain 10 mm wide crack retarders.

Crack retarder surface pretreatment: Using the peel ply, the crack retarder surfaces were modified to optimize the bond quality. Prior to bonding, they were degreased with acetone.

Adhesive bonding: The crack retarders were bonded onto the specimen surface by the Araldite[®] 2011 adhesive. Both specimens were then cured for 24 hours at the ambient temperature and post-cured for 30 minutes at the 80 °C.

3.3 Cold sprayed crack retarders

To compare the bonded crack retarders with the additively manufactured ones, four specimens with cold sprayed crack retarders made of Ti-6Al-4V titanium alpha-beta alloy and AISI 316L austenitic stainless steel were manufactured. Crack retarders were deposited using the Impact Spray System 5/11 and following process parameters: stand-off distance 30 mm, step distance 1 mm, gun travel speed 0.5 m·s⁻¹, gas (N₂) pressure 50 bar and temperature 1100 °C. These process parameters were

chosen according the previous research done by Impact Innovations. To prevent overspray and obtain consistent width and length of crack retarders, the metallic protective mask was utilized prior spraying.

Cold sprayed deposits in as-sprayed condition often possess lower mechanical properties (Fig. 3.3) than wrought counterparts. To increase the load transfer capability, it was decided to increase the height of cold sprayed crack retarders to 0.5 mm and 1.0 mm for both material combinations. After the deposition, the crack retarders were slightly higher and thus their upper surface was milled.

Table 3.3: Mechanical and thermal properties of cold sprayed crack retarder.

Material	Ti-6Al-4V	AISI 316L
E [GPa]	69.7 ^a	182 ^a
ρ [g/cm ³]	4.43 ^b	8.00 ^c
α [10 ⁻⁶ /K]	8.6 ^b	15.9 ^c
Rm [MPa]	295 ^a	795 ^a
$Rp_{0.2}$ [MPa]	-	765 ^a
A [%]	-	0.05 ^a

^a Tested according to ASTM E8.

^b [6]

^c [8]

3.4 Consolidated crack retarders

Two 2024-T351 M(T) specimens with ultrasonically consolidated crack retarders were manufactured. Crack retarders were made of AISI 301 steel; the same composition, thickness and batch as in case of BCRs. Additionally, the 0.05 mm thick interlayer made of 1100 alloy was used between steel layers (Tab. 3.4). The substrate surface had to be machined prior consolidation to be perfectly leveled and clean, for this reason, it was not possible to use the same 2024-T351 bare M(T) specimens as in previous experiments. The crack retarders were first consolidated to the 6 mm thick 2024-T351 sheet and then the M(T) specimen was extracted from the sheet. One 2024-T351 bare M(T) specimen was extracted for the comparison purposes and to avoid batch-to-batch inconsistency.

Table 3.4: Mechanical and thermal properties of 1100-O interlayer used in consolidated crack retarder.

Material	1100-O
E [GPa]	69.0 ^a
ρ [g/cm ³]	2.71 ^a
α [10 ⁻⁶ /K]	23.6 ^a
Rm [MPa]	90 ^a
$Rp_{0.2}$ [MPa]	35 ^a
A [%]	40 ^a

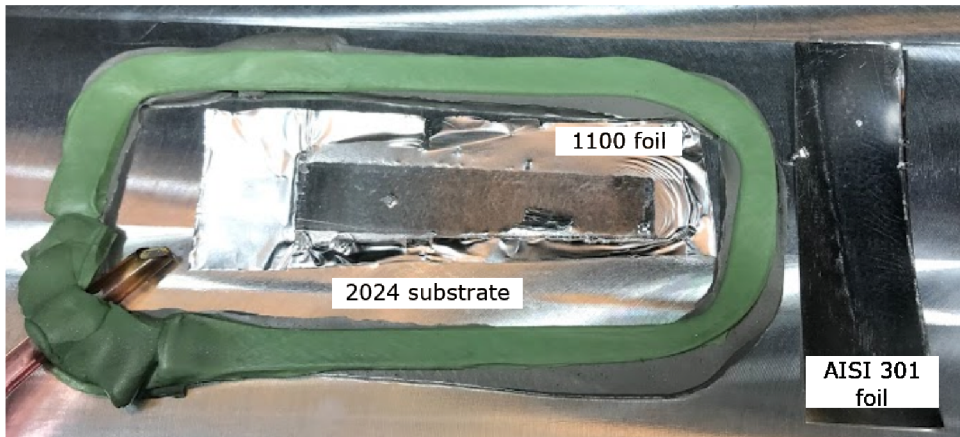
^a [11]

3.4.1 Austenitic stainless steel

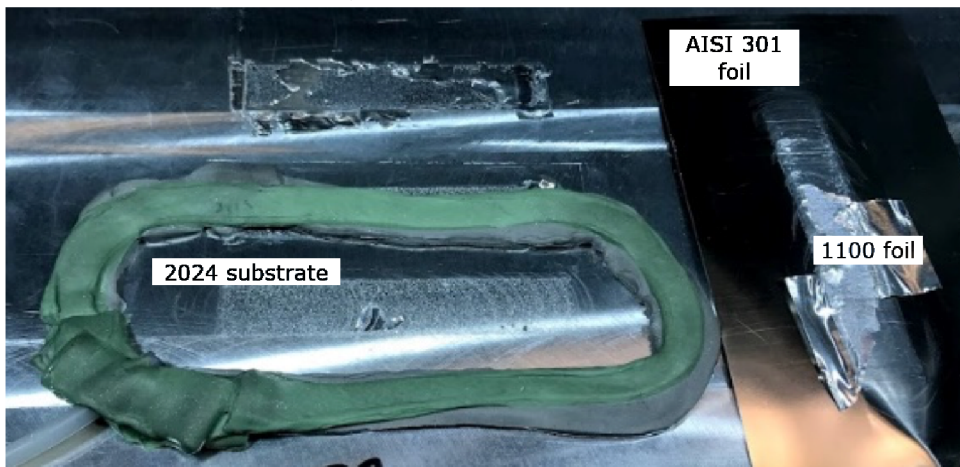
At time of performing experimental studies, consolidating the AISI 301 steel foils of thicknesses 0.255 mm was on the edge of what was possible. Thus the optimal process parameters had to be determined. For this reason, several trials with varying: sonotrode's frequency, longitudinal speed, amplitude, driver³, interlayer thickness were performed by Fabrisonic. The relative strength of the bond between materials was determined using comparative manual peeling test.

The 30 kHz trials were conducted on the Fabrisonic SL 1200, Ultrasonic Additive Manufacturing machine with 2 kW ultrasonic welding system. Across seven trials, the sonotrode's amplitude and interlayer thickness was increasing while the longitudinal speed was decreasing. The pressure in the machine's piston assembly was kept constant at 0.827 MPa; this roughly corresponds to the 3000 N of down force. No bonding to steel was achieved in the Trial 1 (Fig. 3.2a). Based on the results, a good bonding to steel was achieved in the Trial 6, it was moderately hard to peel up steel from anvil (Fig. 3.2b). Some bonding to steel was achieved in the Trial 7, it was difficult to peel up steel from anvil (Fig. 3.2c). Because the results of Trial 6 and 7 were found contradictory, other trials were done.

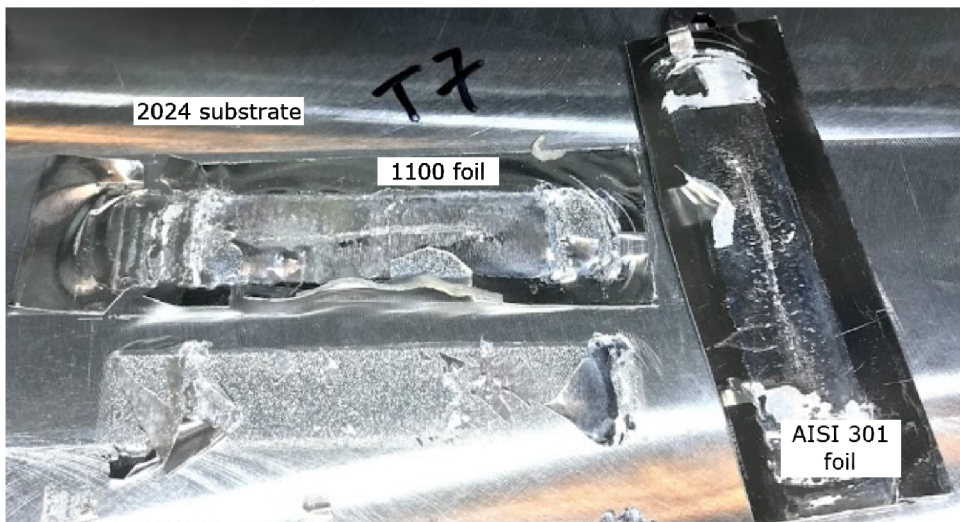
³Driver is placed between sonotrode and foil to be consolidated. Driver holds foil in place, transfers horn's oscillations and prevents foil from bonding to the horn.



(a) Trial 1: 32 μm amplitude, 25.4 mm/s longitudinal speed, titanium driver, 25 μm thick 1100-O interlayer, unheated anvil, 3000 N down force.



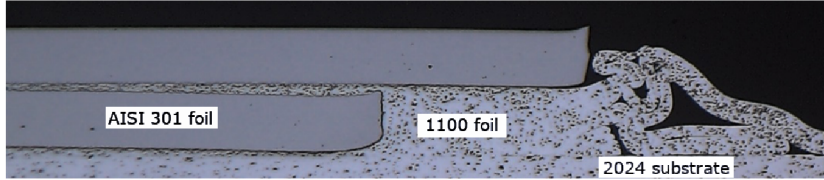
(b) Trial 6: 35.7 μm amplitude, 21.2 mm/s longitudinal speed, no driver, 51 μm thick 1100-O interlayer, unheated anvil, 3000 N down force.



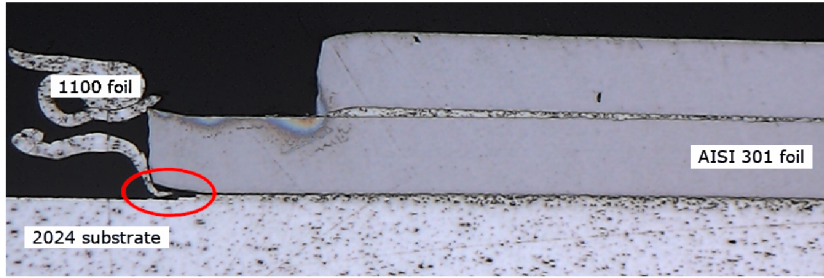
(c) Trial 7: 35.7 μm amplitude, 6.4 mm/s longitudinal speed, titanium driver, 51 μm thick 1100-O interlayer, unheated anvil, 3000 N down force.

Figure 3.2: 20 kHz trials

Two 20 kHz trials were conducted on the Fabrisonic SL 7200, Ultrasonic Additive Manufacturing machine with 9 kW ultrasonic welding system. During these trials, the down force and longitudinal speed were kept constant while the sonotrode's amplitude was increasing. According the results, it was very difficult to peel up steel from anvil in both trials. In the Trial 8, a good bonding to steel was achieved (Fig. 3.3a). However, a few delaminations appeared in the Trial 9 (Fig. 3.3b).



(a) Trial 8: 40 μm amplitude, 21.2 mm/s longitudinal speed, titanium driver, 51 μm thick 1100-O interlayer, anvil heated at 52 $^{\circ}\text{C}$, 7500 N down force.



(b) Trial 9: 41.43 μm amplitude, 21.2 mm/s longitudinal speed, titanium driver, 51 μm thick 1100-O interlayer, anvil heated at 52 $^{\circ}\text{C}$, 7500 N down force. Red circle marks delamination.

Figure 3.3: 30 kHz trials

3.5 Fatigue crack growth test

Prior testing, the 5 mm long notch was machined to the specimen with bonded (CF UD, AISI 301), cold sprayed crack retarders (Ti-6Al-4V, AISI 316L) and without crack retarder (Bare). The 10.6 mm long notch was machined to all specimens with ultrasonically consolidated crack retarders because the precracking was unsuccessful after the 1.0×10^6 - 1.4×10^6 cycles. All specimens with bonded crack retarders, cold sprayed crack retarders, without crack retarder and the specimen with ultrasonically consolidated crack retarders (1-AIS301-UCCR specimen) were subjected to the crack propagation test with the following parameters: $\sigma_{max} = 60$ MPa, $R = 0.1$ and $f = 15$

Hz. Even with the larger machined notch (i.e. 10.6 mm in length), the precracking in the 2-AIS301-UCCR specimen was unsuccessful at the $\sigma_{max} = 60$ MPa and $\sigma_{max} = 80$ MPa. The crack did not start growing after the $1.0 \times 10^6 - 1.4 \times 10^6$ cycles. For this reason, the test was conducted at $\sigma_{max} = 100$ MPa. At this stress level, the fatigue crack started to grow. In all cases, the crack length was periodically measured by the travelling microscope on the specimen's unreinforced side. The cyclic load was applied until the final failure of specimen.

3.6 Delamination monitoring

Delamination monitoring was done by measuring the specimen's thermal response using the Flir SC660 after the optical excitation through 2x 400 W halogen lamps (Fig. 3.4). Thermal response⁴ was collected during heating and decay while the excitation took 5, 7 and 10 seconds. It appeared from the first processed thermal sequences that the highest contrast was acquired after 10 second excitation, so analysis was performed only for this excitation time. To minimize the negative effect of reflective heat, specimens were painted with white spray-paint ThermaSpray 500 with defined emissivity.

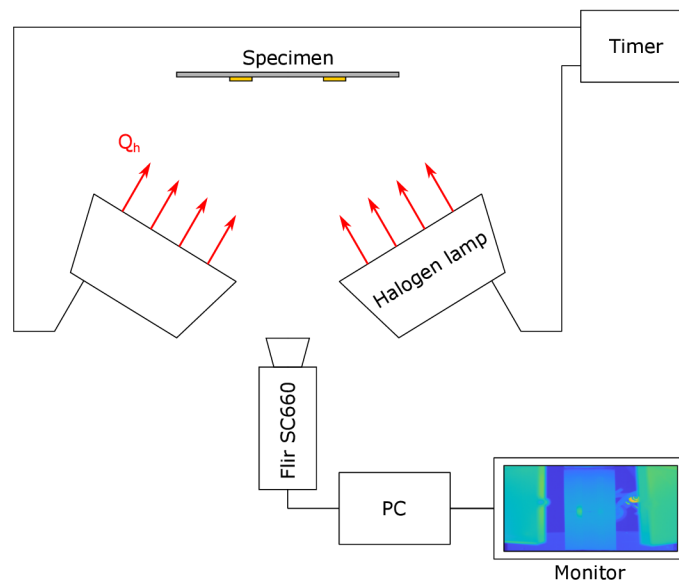


Figure 3.4: Pulsed thermography apparatus.

⁴Sequence of thermal images.

3.7 Digital image processing

Thermal sequence was first normalized to reduce the effect of non-uniform heating and optical properties variability across the measured surface. Then, normalized thermal sequence was fitted with polynomials (i.e. Thermographic Signal Reconstruction) to reduce high spatial frequency noise [12]. Solving the 1st derivative of each polynomial, the flaw to background contrast was increased [12] (Fig. 3.5).

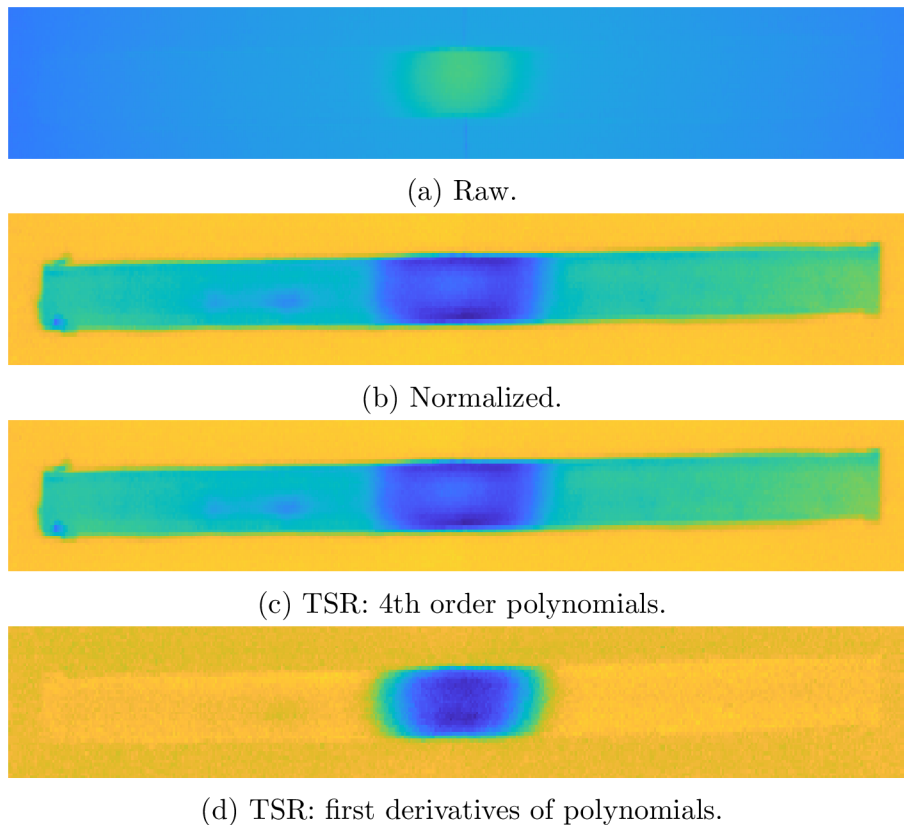


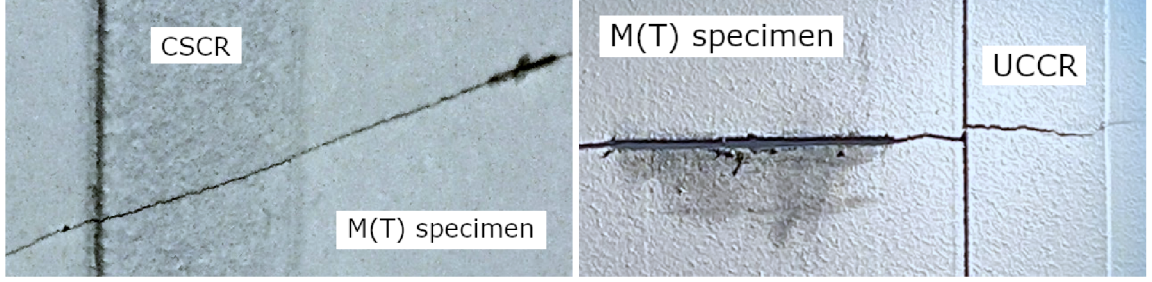
Figure 3.5: Thermographic image processing steps: chronological order.

3.8 Results and discussion

During the crack propagation test, no crack initiation was observed in the BCRs. They broke⁵ or disbond⁶ shortly after the substrate failure. In cases of all cold sprayed crack retarders, the crack propagated directly from the substrate to the crack retarders (Fig. 3.6). In case of the ultrasonically consolidated crack retarders,

⁵1-AISI301A-BCR, 1-CFUD-CR

⁶2-AISI301A-BCR, 2-AISI301B-BCR, 2-CFUD-BCR



(a) Specimen 1-316L-CSCR.

(b) Specimen 1-AISI301-UCCR.

Figure 3.6: Direct propagation of fatigue crack to crack retarder.

the failure was contradictory. The fatigue crack in the specimen with one steel layer (1-AISI301-UCCR) directly propagated to the crack retarder (Fig. 3.6a). However, the crack in the specimen with two steel layers (2-AISI301-UCCR) remained in the substrate and the crack retarders broke immediately after the substrate failure. Measured crack lengths were averaged for each specimen side and plotted against the number of cycles, thus the crack propagation curves were obtained (Fig. 3.7, 3.8).

With regard to specimens possessing crack growth life longer than specimen without crack retarder (Bare), no significant delay can be observed in the crack retarder area, (16–26) mm. The positive crack retarding effect manifests along the entire crack path. Similarly, any significant change in the crack growth rate can be observed in specimens possessing shorter fatigue life.

The fatigue life extension can be expressed by the life extension parameter:

$$LEF = \frac{N_i - N_{bare}}{N_{bare}} \quad (3.1)$$

where N_i is the number of cycles of specimen with crack retarders and N_{bare} is the number of cycles of specimen without crack retarders. All bonded crack retarders resulted in a significant fatigue life extension. The greatest increase, (1.9-2.0), was observed in case of specimen with two steel layers (Fig. 3.9). One can observe a relatively small difference between the fatigue crack growth curves of specimen with two and five CF UD layers. This was probably caused by the evolution of thermal residual stresses during the curing process, which raised the mean stress high enough, to speed-up the crack propagation in the specimen with thicker CF

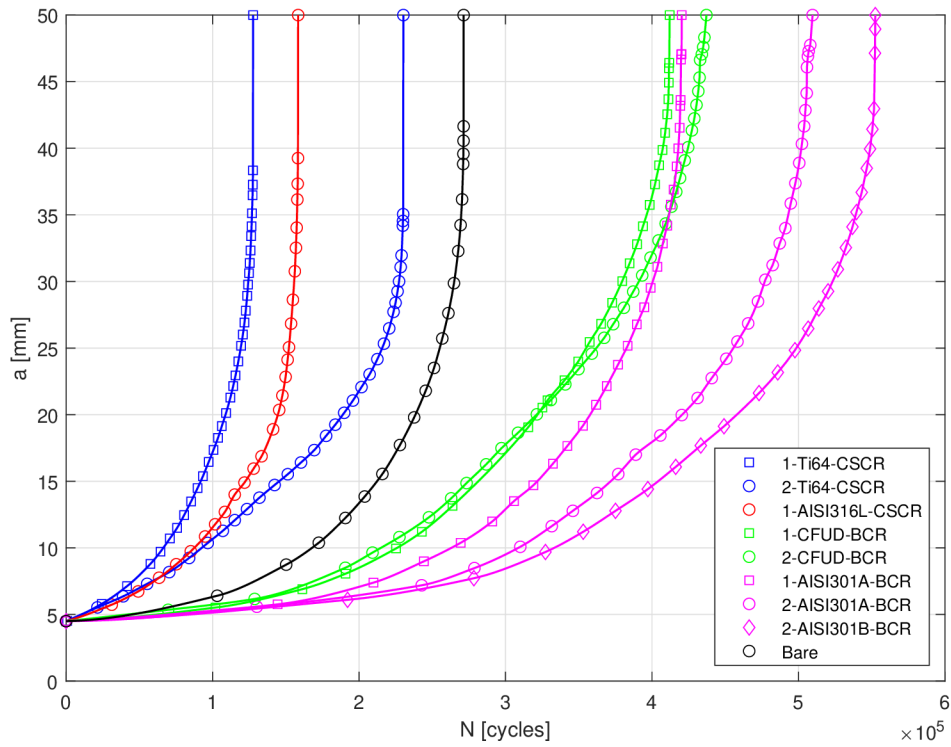
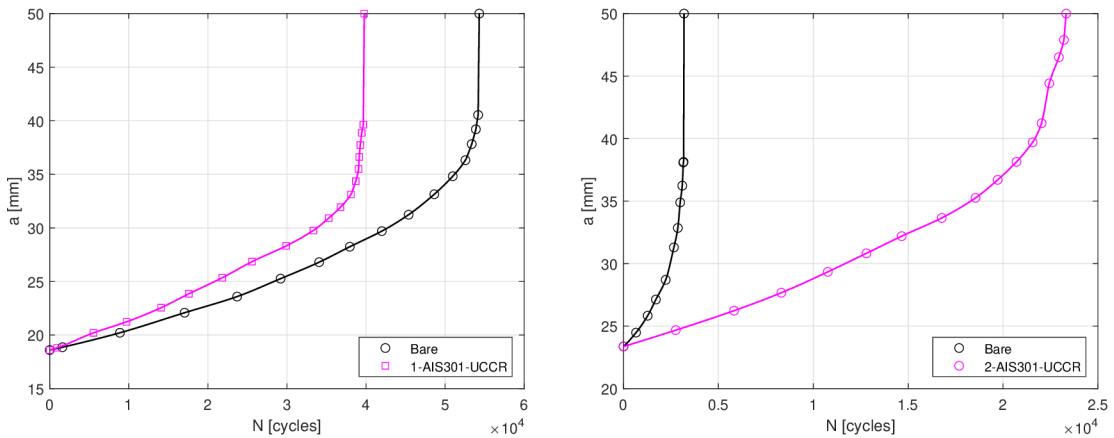


Figure 3.7: Crack growth curves: bonded and cold sprayed crack retarders; $\sigma_{max} = 60$ MPa, $R = 0.1$, $f = 15$ Hz.



(a) 1-AISI301-UCCR specimen.

(b) 2-AISI301-UCCR specimen.

Figure 3.8: Crack growth curve: ultrasonically consolidated crack retarders; $R = 0.1$, $f = 15$ Hz.

UD crack retarders. Regarding this observation, using more than two CF UD layers appears to be redundant. All cold sprayed crack retarders dramatically decreased the fatigue life. The greatest decrease, 50%, was observed in the fatigue life of specimen with the Ti-6Al-4V crack retarders. The specimen with the thicker 316L crack retarder failed within the crack initiation period due to the presence of rapidly growing crack at one of the ends of the crack retarder.

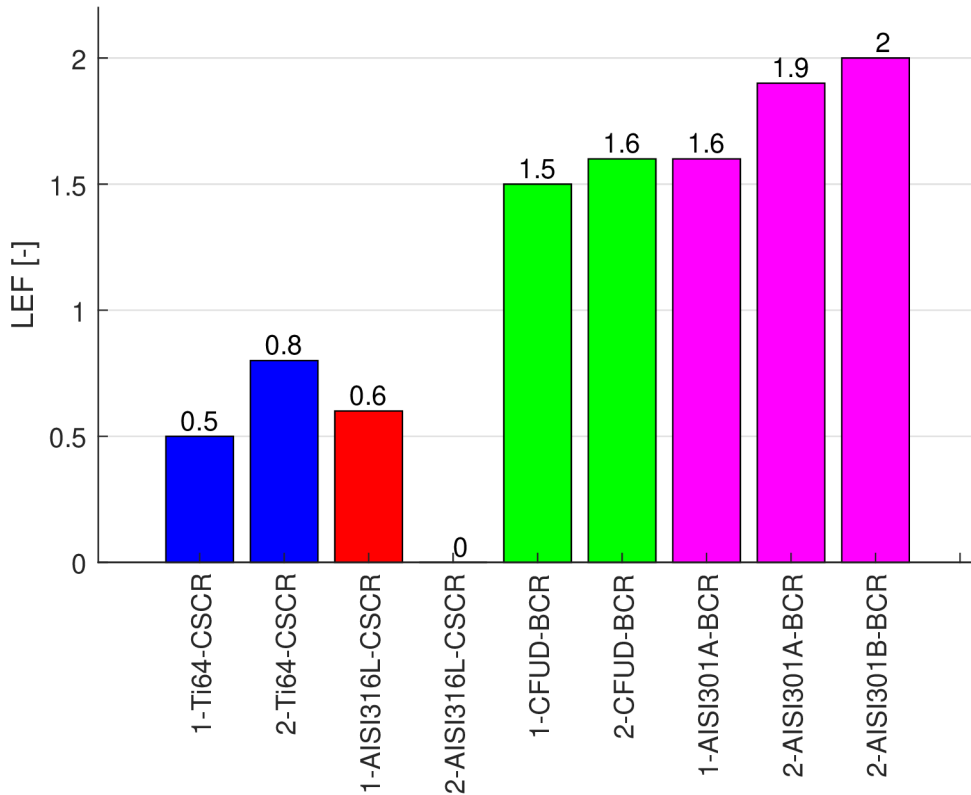
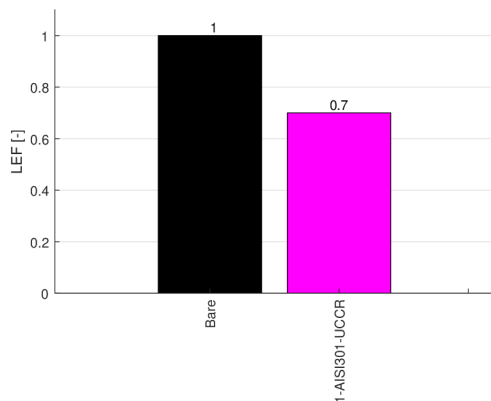


Figure 3.9: Life extension parameter: bonded and cold sprayed crack retarders.

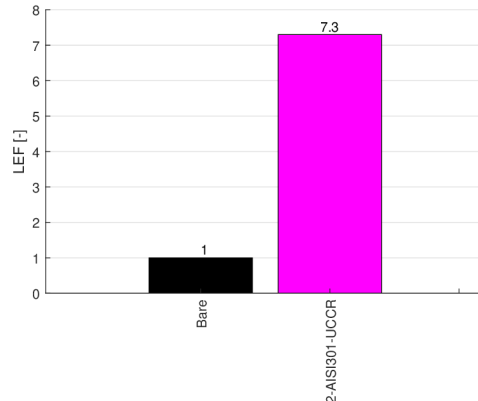
Regarding the poor fatigue properties (i.e. decreased fatigue life and increased crack growth rate) of specimens with CSCRs, there are several explanations. The substrate temperature increased due to its plastic deformation during cold spraying and due to the heat transfer from the impinging jet. A combination of cooldown from such temperature and the crack retarder's CTE dissimilar from the substrate probably led to the evolution of tensile residual stresses in the substrate. The typical out-of-plane deformation was observed in all specimens with CSCRs [13]. The temperature increase in the substrate certainly altered its mechanical properties.

A noticeable drop in the substrate hardness was measured in all specimens with CSCRs. Additionally, the crack retarder failed prematurely due to the poor fatigue properties of as-sprayed crack retarders. The poor fatigue properties of cold sprayed deposits were also observed by Čížek et al. [14]. In their study, the pure metallic specimens (Ti, Ni, Al, Cu) possessed greater fatigue crack growth rates than cold-rolled counterparts.

Specimen with one ultrasonically consolidated steel layer (1-AISI301-UCCR) failed earlier, thus his fatigue life was 30% lower compared to the specimen without crack retarder (Bare) (Fig. 3.10a). However, specimen with two steel layers (2-AISI301-UCCR) experienced the greatest increase by a factor of 7.3 (Fig. 3.10b). Note that in this specimen, the precrack length was five times greater and the σ_{max} was 1.66 times greater compared to the specimens with bonded and cold sprayed crack retarders.



(a) 1-AISI301-UCCR specimen.



(b) 2-AISI301-UCCR specimen.

Figure 3.10: Life extension parameter.

To obtain crack growth rates, the fatigue crack growth data were interpolated using the Modified Akima piecewise cubic Hermite interpolation spline (makima). Since the beginning of the test, the specimens with CF UD and steel bonded crack retarders maintained the crack growth rate below the growth rate of bare specimen (Fig. 3.11). Unfortunately, the specimens with cold sprayed crack retarders possessed a higher rate in the whole crack length range, which resulted in already mentioned shorter fatigue life. Although, the crack retardation in the specimen 2-Ti64-CSCR can be identified in the (11–28) mm crack length range, the specimen

failed earlier than the bare one because the crack grew significantly faster in other regions. The fatigue crack growth rate in specimen with one steel layer (1-AISI301-UCCR) was higher in the whole crack length range (Fig. 3.12a), which resulted in already mentioned shorter fatigue life. On contrary, the specimen with two steel layers possessed fatigue crack growth rate significantly lower compared to the specimen without crack retarders (Fig. 3.12b).

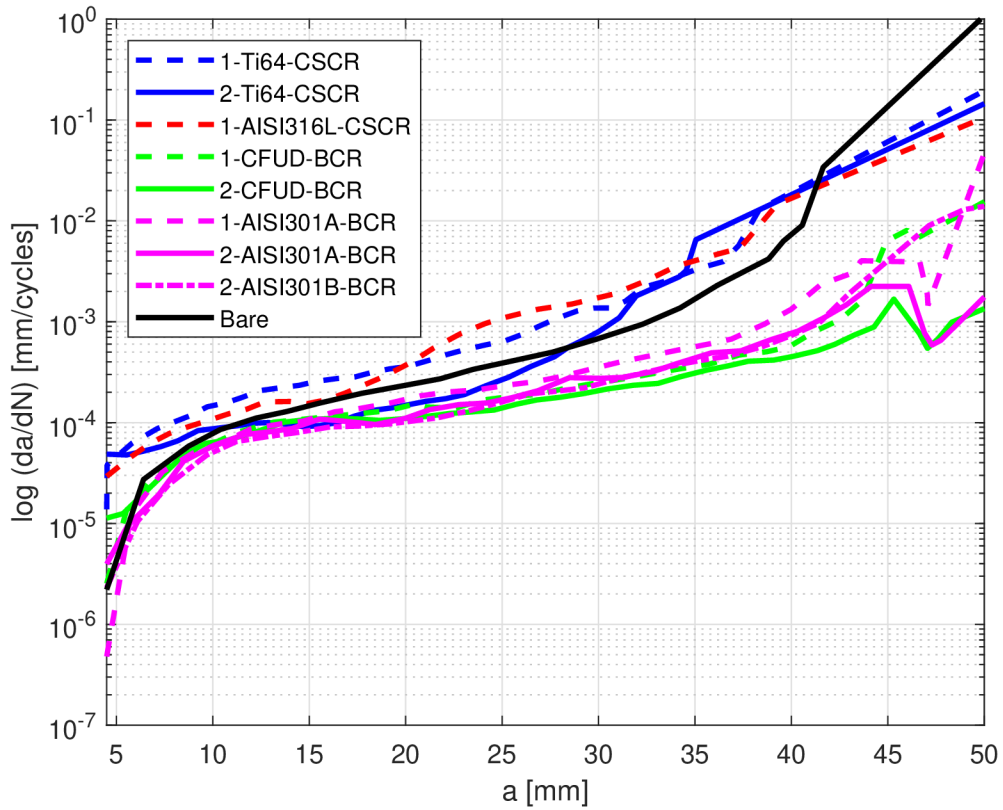
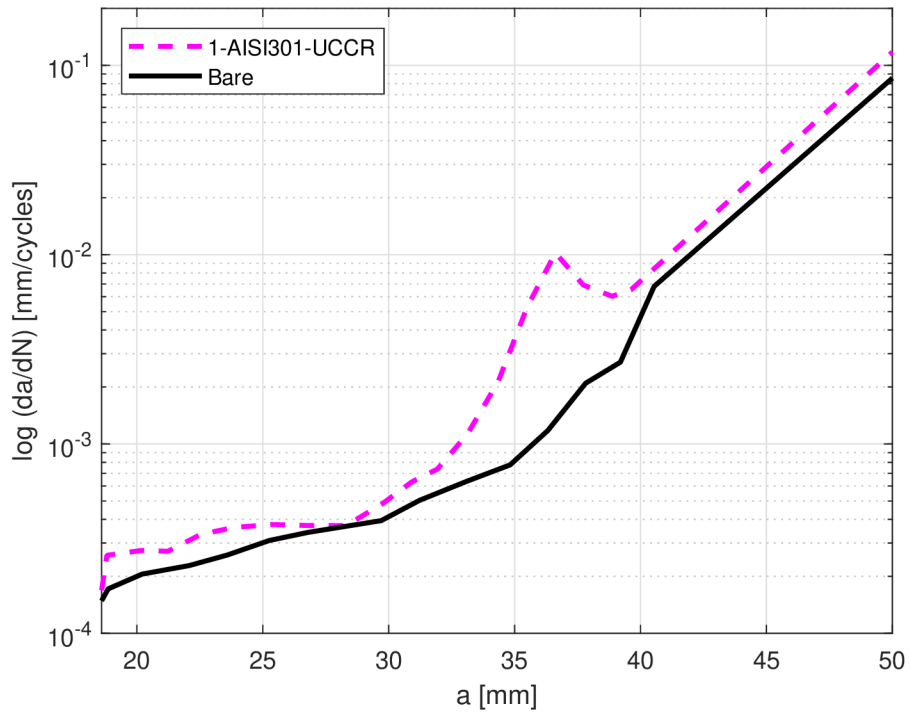


Figure 3.11: Fatigue crack growth rate: bonded and cold sprayed crack retarders.

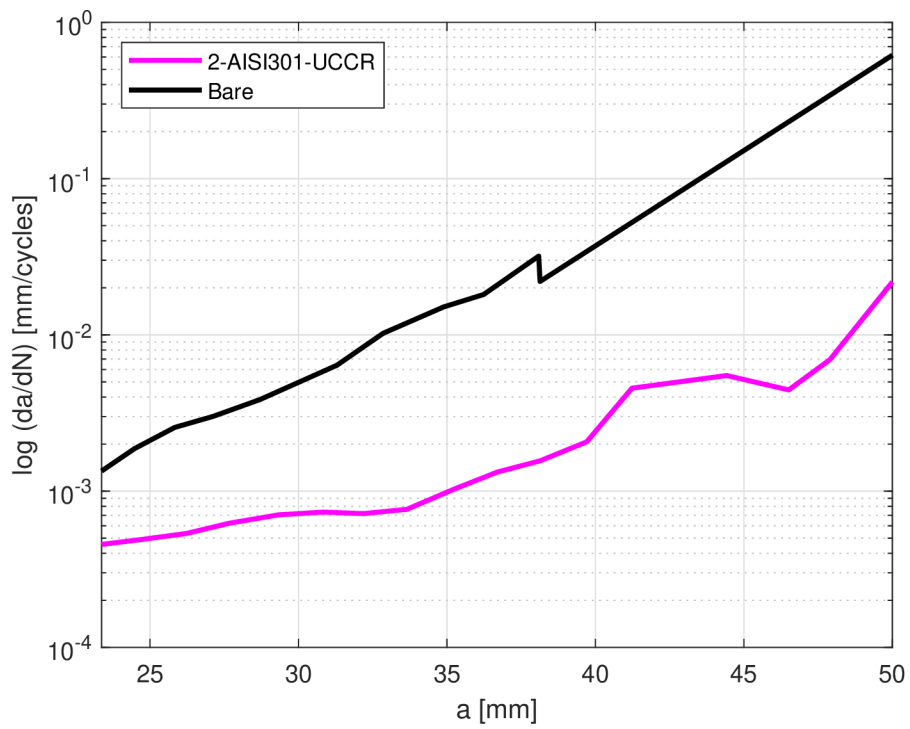
The percentage of life improvement with respect to the bare specimen per gram weight of crack retarder can be expressed by a subsequent parameter [3]:

$$e = \frac{N_i - N_{bare}}{N_{bare}} \frac{100}{m_{strap}} \quad (3.2)$$

where m_{strap} is the crack retarder weight. It is obvious that the BCR made of two CF UD layers can significantly extend fatigue life while maintaining relatively low weight of a specimen (Fig. 3.13). One can also observe that the thinner BCR were



(a) 1-AISI301-UCCR specimen.



(b) 2-AISI301-UCCR specimen.

Figure 3.12: Fatigue crack growth rate: ultrasonically consolidated crack retarders.

much more effective than the thicker ones, however, this fact was already proved by Boscolo [3] and Molinari [15]. Specimens with steel BCRs did not perform in the same way. In comparison with carbon fibre crack retarders, their total thickness was lower. They probably did not experience the secondary bending to the extent that would have led to the lower performance. The greatest life increase with respect to the crack retarder unit weight, $82.2\% g^{-1}$, was observed in the ultrasonically consolidated crack retarder with two steel layers (2-AISI301-UCCR)⁷.

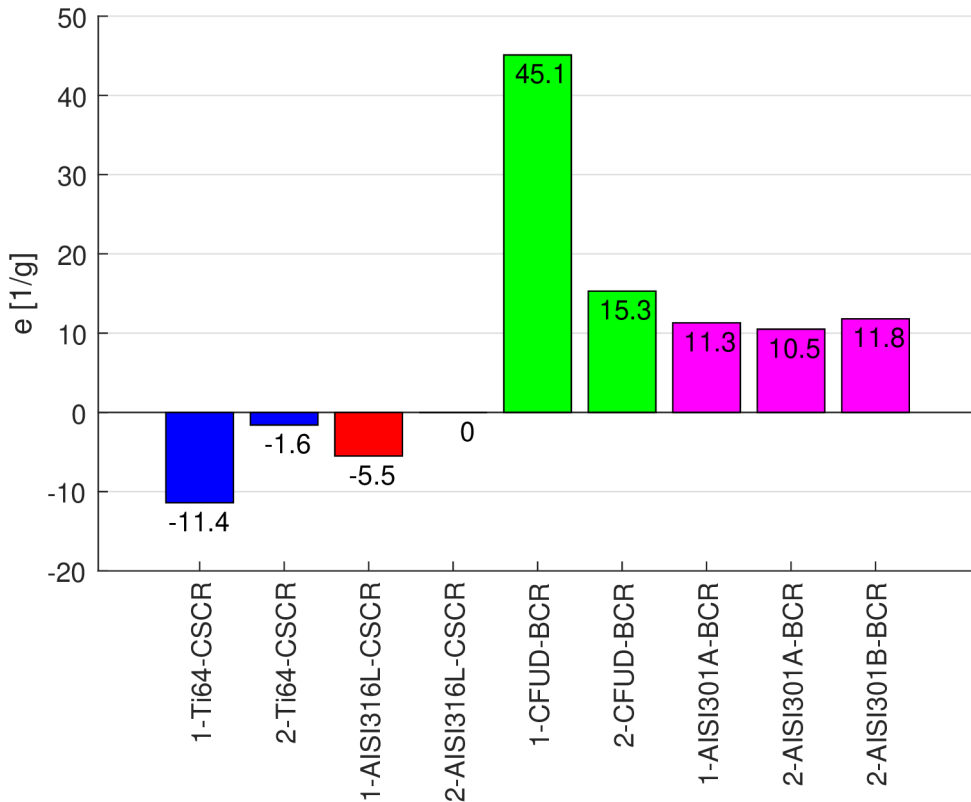


Figure 3.13: e factor: bonded and cold sprayed crack retarders.

All bonded crack retarders started delaminating in the end of specimen's fatigue life. The delamination in specimens with carbon fibre BCRs started later compared to the delamination in specimens with steel BCRs (Fig. 3.14). The steel crack retarders delaminated with continually increasing delamination rate. The earlier onset of delamination in specimens with steel crack retarders can be attributed to

⁷In this specimen, the precrack length was five times greater and the σ_{max} was 1.66 times greater compared to the specimens with bonded and cold sprayed crack retarders.

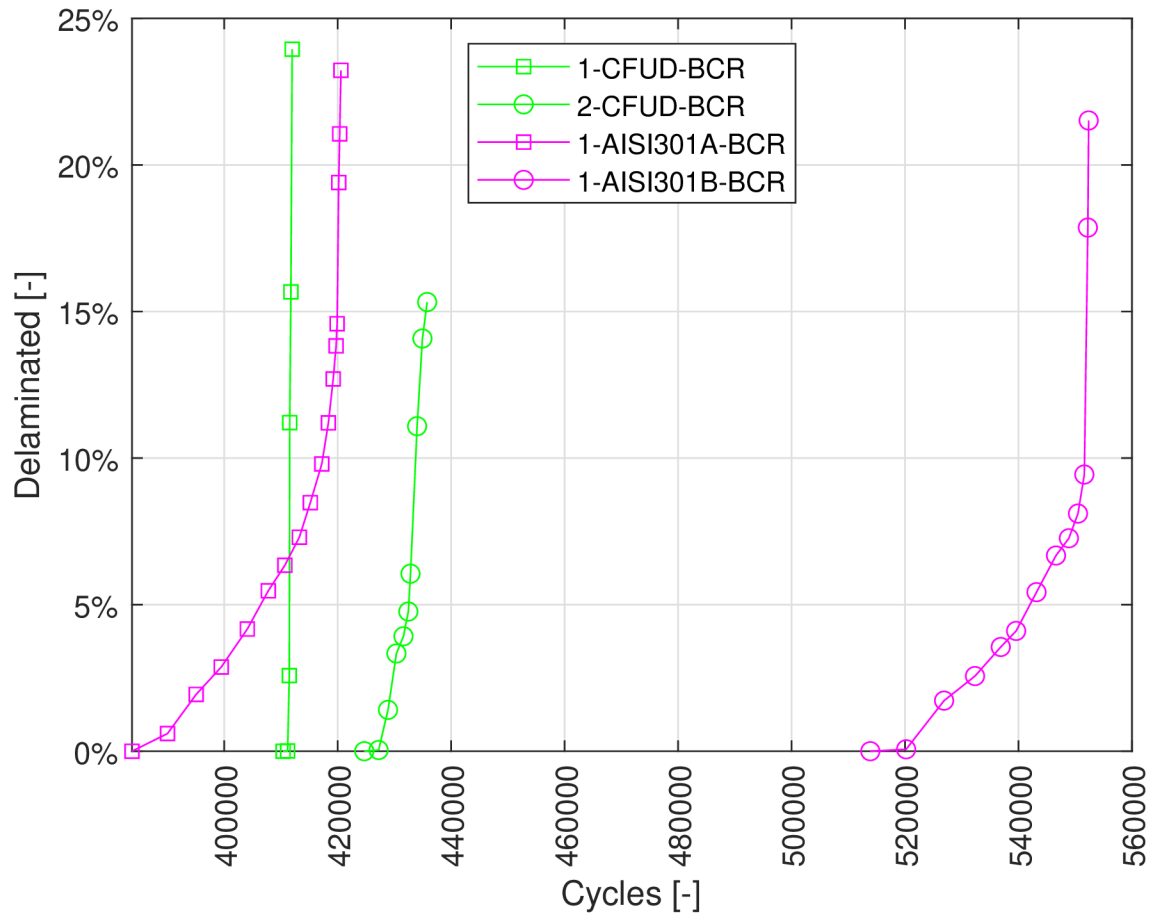


Figure 3.14: Delamination growth: bonded crack retarders.

the weaker joint strength. The fracture surface between CF UD crack retarder and substrate showed adhesive-cohesive failure. Conversely, fracture surface between steel crack retarder and substrate was purely adhesive failure. This suggests that if the joint strength (AISI 301/substrate) is increased, the fatigue retardation effect may be increased. The crack grew directly to the crack retarder without premature delamination in all specimens with cold-sprayed crack retarders. Samely, ultrasonically consolidated crack retarder with one steel layer (1-AISI301-UCCR) did not delaminate, the crack grew directly into him. However, the delamination in ultrasonically consolidated crack retarder with two steel layers (2-AISI301-UCCR) followed the same trend as the bonded crack retarders (Fig. 3.15); two steel layers start to delaminate in the end of specimen's fatigue life.

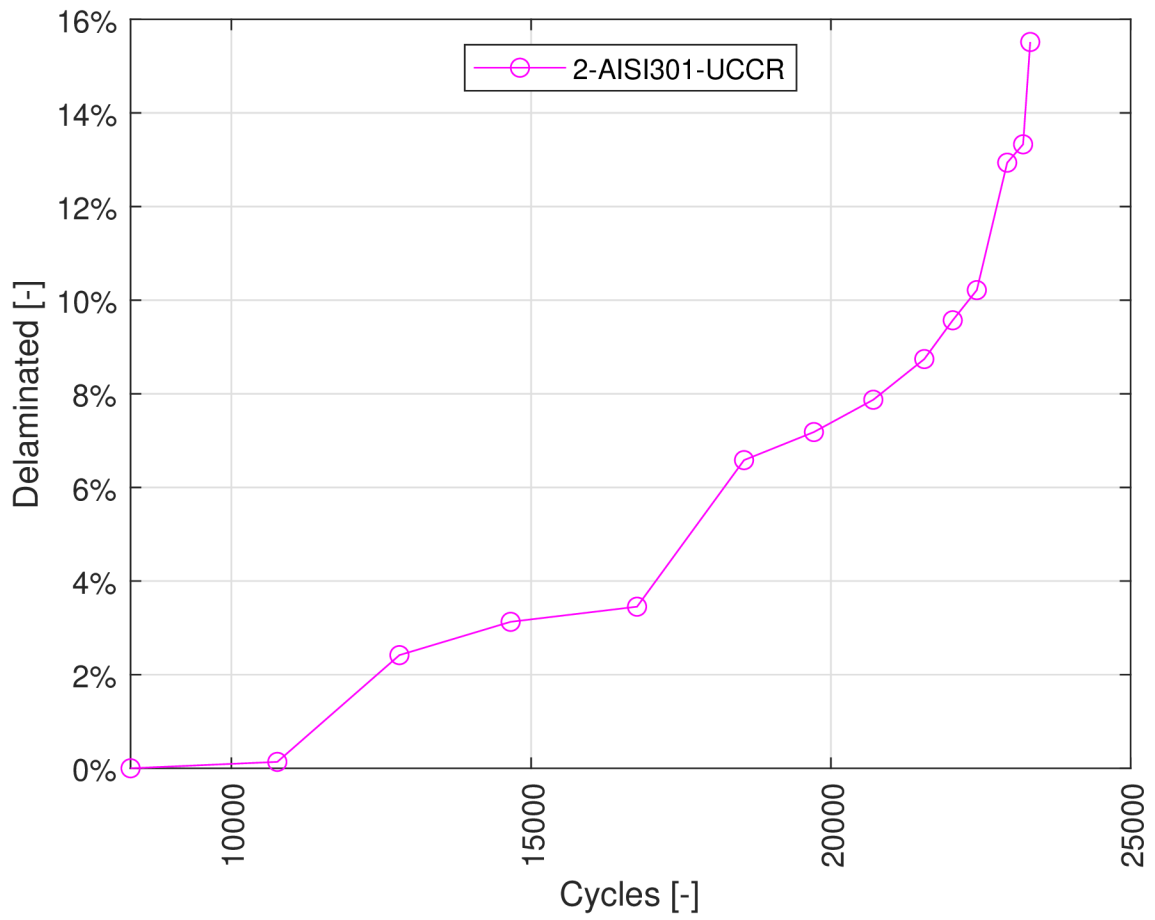


Figure 3.15: Delamination growth: 2-AISI301-UCCR specimen.

Chapter 4

Conclusion

From the results discussed in the previous chapter, the following conclusions can be drawn:

- Fatigue life of aluminum structure can be significantly improved using the bonded crack retarders made of AISI 301, CF UD/epoxy and ultrasonically consolidated crack retarders made of AISI 301/Al. The greatest increase by a factor 7.2 was recorded in specimen with ultrasonically consolidated AISI 301/Al crack retarder.
- Utilizing bonded CF UD, AISI 301 crack retarders or ultrasonically consolidated AISI 301/Al crack retarder; the fatigue crack growth rate in the aluminum structure can be significantly decreased.
- The greatest percentage of life improvement with respect to the bare specimen per gram weight of crack retarder, 82.2% g^{-1} , was detected in the specimen with ultrasonically consolidated AISI 301/Al crack retarder.
- The delamination in AISI 301/Al laminate can be recorded using pulsed thermography. Thermographic signal reconstruction method proved to be a relevant approach to increase the contrast of delamination in ultrasonically consolidated AISI 301/Al laminate.
- The delamination growth between ultrasonically consolidated AISI 301/Al crack retarder and aluminum structure follows the same trend as delamination

between the bonded crack retarder and aluminum structure. The delamination patterns of bonded and ultrasonically consolidated crack retarders possess the similar shape.

4.1 Research implication and contribution

4.1.1 Practical

Through the application of crack retarder, the fatigue crack can experience stable growth for longer period of time. In other words, the critical crack length increases and thus the:

- aircraft maintenance interval will be longer [16]
- time to the first inspection (i. e. inspection threshold) will be longer [16]
- number of inspection might be reduced if maintenance tasks are fittingly associated
- crack detectability increases, since longer cracks are always easier to detect

A high-performance cars, boats and spacecrafts are other candidates that could benefit from the application of crack retarders. The crack retarder's influence to load capacity, fracture toughness, buckling resistance and residual strength was not examined in this thesis, however, the positive impact on all these structural properties is strikingly obvious because of the stiffening effect.

4.1.2 Scientific

This thesis (1) compares the impact of novel material combinations and technologies on the fatigue crack growth rate and the delamination growth; (2) brings the experimental data for the calibration of predictive models that may involve the delamination growth; (3) marks the potential dead end, i.e. the cold spray deposit might increase the fatigue crack growth rate and thus decrease the fatigue life; (4) proves that the delamination in the ultrasonically consolidated metal laminates can be detected using the pulsed thermography.

References

- [1] G. I. Nestrenko, “Comparison of damage tolerance of integrally stiffened and riveted structures,” in *22nd International Congress of Aeronautical Sciences*, 2000.
- [2] S. Findlay and N. Harrison, “Why aircraft fail,” *Materials Today*, vol. 5, no. 11, pp. 18–25, 2002, ISSN: 1369-7021. DOI: 10.1016/S1369-7021(02)01138-0.
- [3] M. Boscolo, G. Allegri, and X. Zhang, “Design and modelling of selective reinforcements for integral aircraft structures,” *AIAA journal*, vol. 46, no. 9, pp. 2323–2331, 2008.
- [4] M. C. Dixon, *The Maintenance Costs of Aging Aircraft: Insights from Commercial Aviation*. Santa Monica, CA: RAND Corporation, 2006.
- [5] *Standard test method for measurement of fatigue crack growth rates*, <https://www.astm.org/standards/e647>, Accessed: 2022-03-10.
- [6] *ASM Handbook, Volume 2: Properties and selection: Nonferrous alloys and special-purpose materials*. Materials Park, Ohio: ASM International, 1990, ISBN: 978-0-87170-378-1.
- [7] P. Dymáček and J. Klement, “Properties and manufacturing of steel-C/epoxy fiber-metal laminates,” in *Proceedings of the Fourth Seminar on Recent Research and Design Progress in Aeronautical Engineering and its Influence on Education: Part II*, Institute of Aeronautics and Applied Mechanics, 2011, pp. 47–52.
- [8] *ASM Handbook, Volume 1: Properties and Selection: Irons, Steels, and High-Performance Alloys*. Materials Park, Ohio: ASM International, 1990, ISBN: 978-0-87170-377-4.
- [9] *HexPly® M10R*, Hexcel, 2015.
- [10] *Araldite® 2011 (AW106 + HW953U): Two component epoxy paste adhesive*, Huntsman Advanced Materials, 2004.
- [11] *ASM Specialty Handbook: Aluminum and Aluminum Alloys*. Materials Park, Ohio: ASM International, 1993, ISBN: 978-0-87170-496-2.
- [12] S. M. Shepard and M. F. Beemer, “Advances in thermographic signal reconstruction,” in *Thermosense: thermal infrared applications XXXVII*, International Society for Optics and Photonics, vol. 9485, 2015, 94850R.
- [13] C. Liljedahl, M. Fitzpatrick, and L. Edwards, “Distortion and residual stresses in structures reinforced with titanium straps for improved damage tolerance,” *Materials Science and Engineering: A*, vol. 486, no. 1-2, pp. 104–111, 2008.
- [14] J. Cizek, O. Kovarik, J. Cupera, *et al.*, “Measurement of mechanical and fatigue properties using unified, simple-geometry specimens: Cold spray additively manufactured pure metals,” *Surface and Coatings Technology*, vol. 412, p. 126 929, 2021, ISSN: 0257-8972. DOI: 10.1016/j.surfcoat.2021.126929.

- [15] G. Molinari, I. Meneghin, M. Melega, and E. Troiani, "Parametric damage tolerance design of metallic aeronautical stiffened panels," *The Aeronautical Journal*, vol. 116, no. 1182, pp. 815–831, 2012.
- [16] D. Vlcek, *Damage tolerance evaluation of L410 NG aircraft lower wing integrally stiffened panel*, Section: Detectability and inspection program, 2013.

Abbreviations

BCR Bonded Crack Retarder

BCRs Bonded Crack Retarders

CF Carbon Fibre

CSCR Cold Sprayed Crack Retarders

FPL Forest Products Laboratory

makima Modified Akima piecewise cubic Hermite interpolation Matlab Function

UCCR Ultrasonically Consolidated Crack Retarder

UD Unidirectional

EDUCATION

Brno University of Technology Master's degree Ing. – Specialization: Aircraft Design	Brno 2014–2016
Brno University of Technology Bachelor's degree Bc. – Specialization: Mechanical Engineering	Brno 2011–2014
SPŠ a VOŠ Brno, Sokolská High school – Specialization: Computer Graphics	Brno 2007–2011

EXPERIENCE

Brno University of Technology R&D Mechanical Engineer	Brno 2018–Current
---	----------------------

TEACHING

- **Teaching Assistant** at Brno University of Technology
Aircraft Manufacture I, Aircraft Manufacture II 2016–2018

SCHOLARSHIPS AND AWARDS

- Scholarship for outstanding study results 2012
- Pass with Distinction 2016

OTHER ACADEMIC ACTIVITIES

- Reviewer for International Journal of Fatigue 2021–Current

PUBLICATIONS

1. JETELA, V.; KLEMENT, J.; AUGUSTIN, P. Possibility for improving damage tolerance of integral structure by high strength bonded straps. *Manufacturing TECHNOLOGY*, 2018, roč. 18, č. 4, s. 572-577. ISSN: 1213-2489.
2. JETELA, V. Bonded Crack Retarders: A review. In *Nové Trendy v Civilnom Letectve*. Bratislava: EDIS - vydavateľské centrum Žilinskej univerzity, 2019. s. 77-81. ISBN: 978-80-554-1579-6.
3. JETELA, V.; KLEMENT, J.; AUGUSTIN, P. Possibility for improving damage tolerance of integral structure by high strength bonded straps. In *14th Seminar "Materials and technologies in Special Technics Production 2017"*. Brno: University of Defence, 2017. s. 29-33. ISBN: 978-80-7231-420-1.